INVESTIGATION OF FAILURE OF HIGH BURN UP CARBIDE FUEL PIN OF FBTR THROUGH POST-IRRADIATION EXAMINATION

V. KARTHIK, RAN VIJAY KUMAR, V.V. JAYARAJ, V. ANANDRAJ, B.K. OHJA, C. PADMAPRABU, A.VIJAYARAGAVAN, T. ULAGANATHAN, C.N. VENKITESWARAN, SHAJI KURIEN, T. JOHNY, R. DIVAKAR, JOJO JOSEPH, S. VENUGOPAL AND T. JAYAKUMAR

Metallurgy and Materials Group
Indira Gandhi Centre for Atomic Research
Kalpakkam 603102, India

ABSTRACT

A fuel pin failure was identified for the first time in the mixed carbide fuelled Fast Breeder Test Reactor (FBTR) at a burn-up of 148.3 GWd/t. Post irradiation examinations were carried out on the failed fuel subassembly in the hot cells to investigate and analyse the causes of failure. The investigations included a series of non-destructive examination techniques like X ray & neutron radiography, axial gamma scanning, and profilometry on select intact pins as well as the failed pin. Based on the results, a few fuel pins were selected for fission gas analysis, metallography, high temperature tensile testing of cladding and clad swelling measurements. The results obtained were compared with that of fuel pins which had reached a burn-up of 155 GWd/t without failure under similar irradiation conditions.

The failure of the cladding in the form of a longitudinal rupture is attributed to be the combined effect of high radial and axial stresses in the clad resulting from high Fuel Clad Mechanical Interaction (FCMI) and local bending of a few pins in the failure region. The failed pin and adjacent pins have evidently been subjected to high temperatures, presumably due to local coolant flow reduction between two pins that came closer as a result of local bending.

1.0 Introduction

The 40MWt Fast Breeder Test Reactor (FBTR) at Kalpakkam, India, has been in operation with helium bonded mixed carbide fuel of composition $(U_{0.3}, Pu_{0.7})C$ as the driver fuel and 20% cold worked AISI 316 as the core structural material. So far, more than 1500 carbide fuel pins have achieved a peak burn-up of 155 GWd/t at a peak linear heat rating (LHR) of 400 W/cm. Performance assessment of the carbide fuel and AISI 316 clad/wrapper has been carried out through post-irradiation examinations (PIE) at various stages starting from beginning of life conditions (1000 MWd/t) up to a peak burn-up of 155 GWd/t. [1, 2]

Failure of a fuel pin in FBTR was identified for the first time based on increased cover gas activity and delayed neutron signals. One carbide fuel subassembly (FSA) in the third ring of FBTR with a burn-up of 148.3 GWd/t was identified to have pin failure and was subsequently subjected to detailed PIE in hot cells of Radiometallurgy laboratory to identify the causes of failure. The details of the investigation and the results obtained are presented in this paper.

2.0 Irradiation history

The typical peak linear heat rating (LHR) of the fuel pins in the failed FSA was around 280 W/cm as compared to the peak LHR of 385 W/cm close to the FBTR core center. The subassemblies had operated at higher sodium inlet and outlet temperatures after a burn-up of 125 GWd/t till failure due to a change in the reactor configuration. The calculated clad mid-wall temperatures correspondingly increased from 350°C (core bottom)/510°C (core top) to 380°C/585°C. The peak displacement damages were estimated to be around 87 dpa NRT.

3.0 Identification of the failed pin(s)

Visual examination of the failed fuel subassembly (FFSA) did not indicate any significant abnormalities on its external surfaces. The FFSA was subjected to sodium removal and metrological measurements followed by cutting the the foot portion with Nd:YAG laser tool. The bundle of 61 fuel pins was carefully extracted and all the fuel pins were visually examined and one fuel pin was identified with a longitudinal rupture of ~70mm length starting at 172 mm from top of the pin (Fig.1). Leak testing was performed on the remaining pins using thermal conductivity based Helium gas leak detector by bombing and sniffing method. Leak testing confirmed that the remaining pins were intact with leak rate better than 10^{-3} std cc/sec.

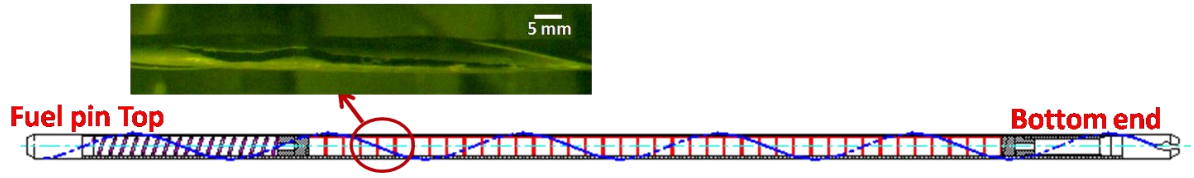

Fig 1. Photograph of the failed fuel pin and its axial location

4.0 Detailed examinations to assess the cause of failure

In addition to the failed pin, twelve intact pins were selected for comprehensive examinations based on their proximity to the failed pin and the extent of displacement damage seen by them (Fig. 2). Investigations were planned to assess the condition of the fuel and clad for signatures of impending failure, if any. Non-destructive examination techniques performed to characterise the intact pins and failed pin included neutron radiography, axial gamma scanning, and profilometry. Based on the results obtained, a few fuel pins were selected for further examination through fission gas analysis, metallography, high-temperature tensile testing of cladding and clad swelling measurements. The failed location of the pin was subjected to fractography, metallography and microhardness measurements. The results obtained were compared with that obtained for a I[st] ring FSA and another III[rd] ring FSA that had reached a burn-up of 155 GWd/t without failure. The experimental details of the various PIE techniques employed in this study are described elsewhere [3, 4]. The salient results of the investigations are presented in the following section.

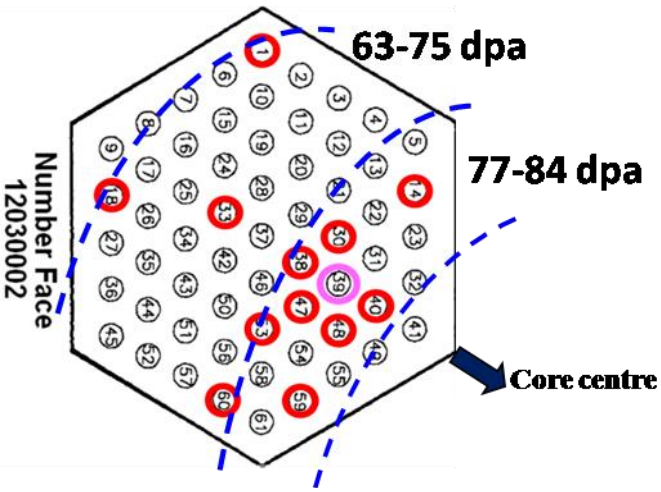

Fig 2. Schematic showing the fuel pins selected (encircled) for detailed examinations. Pin 39 is the failed pin location

5.0 Results

5.1 Fuel pin metrology and clad swelling

The fuel pin diameter measurements indicated maximum dilation around the centre of fuel column corresponding to peak fluence region. There was no measurable diameter increase in the top and bottom plenum locations of the fuel pins. The diameters of the failed pin at different axial locations (away from the failure region) were in the same range as that of the neighbouring fuel pins. Table 1 gives the range of diameter and length increase of the 12

fuel pins of FFSA. It was seen that the increase in length and diameter of the fuel pins of FFSA were in general higher than the pins of FSA $_{\text{I ring-155 GWd/t}}$ of similar peak displacement damages. The failed fuel pin and surrounding pins show localised bending at the same axial locations as that of failure (Fig. 3). Fuel pins of higher diametral strains exhibited asymmetrical deformation (in two perpendicular orientations), in addition to bending.

Dimensional changes of fuel pins	Diameter Increase (mm)	Length Increase (mm)
FFSA (12 Pins)	0.185 - 0.320	2.49 - 5.92
FSA$_{\text{I ring-155 GWd/t}}$ (13 pins)	0.180 - 0.270	1.90 - 4.28

Table 1: Summary of the diameter and length increase of the fuel pins of FFSA compared with that of the pins of FSA $_{\text{I ring-155 GWd/t}}$

The swelling and creep components of the diamteral strain of cladding were decoupled by estimating swelling strain ($\frac{1}{3}\Delta V/V$) from density measurements [5]. For the pins of FFSA, the swelling component was low (Fig. 4) as compared to the pins of FSA $_{\text{I ring-155 GWd/t.}}$ The higher creep contribution to the diametral strain suggests high clad stresses due to Fuel Clad Mechanical Interaction (FCMI) in the pins of FFSA.

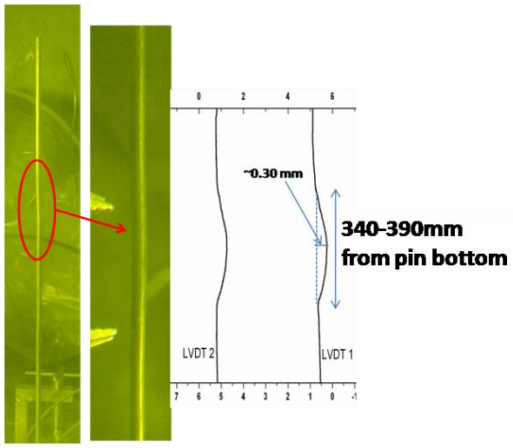

Fig 3. Photograph of typical fuel pin and its LVDT trace showing localized bending

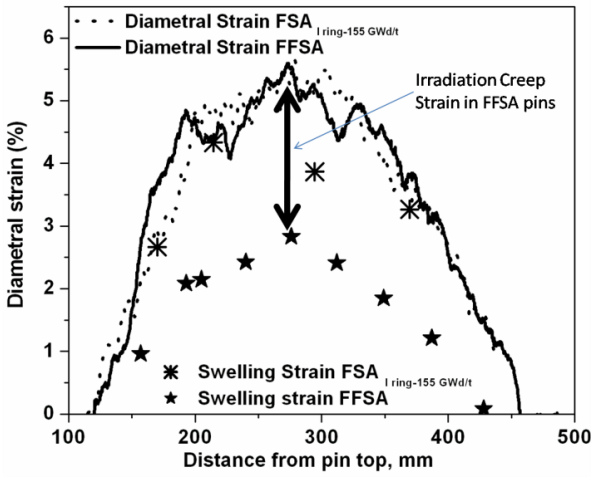

Fig 4. Relative contribution of swelling and irradiation creep components to the total diametral strain

5.2 Radiography

Neutron radiography carried out using indirect transfer technique revealed adherence of the remnant fuel to the inner surface of the cladding indicating strong bonding of the fuel with clad. Stack length increase measured by X-ray and neutron radiography indicated higher increase (12-16mm) compared to 9 - 12 mm observed in pins of FSA$_{\text{I ring-155GWd/t}}$, indicating higher fuel swelling in pins of the failed FSA. Local bending of fuel pins was observed in the X-ray and neutron radiographs in the failed pin and other fuel pins in the region corresponding to the failed location.

5.3 **Fission product migration and fission gas release**

Axial distribution of the fission products (FP) in the fuel pins was evaluated with particular attention to FPs ^{137}Cs, which is known to migrate down the temperature gradients, and ^{106}Ru which does not have a tendency to migrate.

Extensive perturbation in the profile of Cesium isotope (^{137}Cs) at axial locations starting near the peak power location was observed in the failed pin. Similar perturbations in Cs profile was observed in fuel pins adjacent to the failed pin while fuel pins located away from the failed pin did not indicate any such perturbations (Fig. 5). The extent of migration and redistribution was severe in fuel pins surrounding the failed fuel pin pointing to the possibility of higher fuel temperatures in the fuel pins in the region of failure.

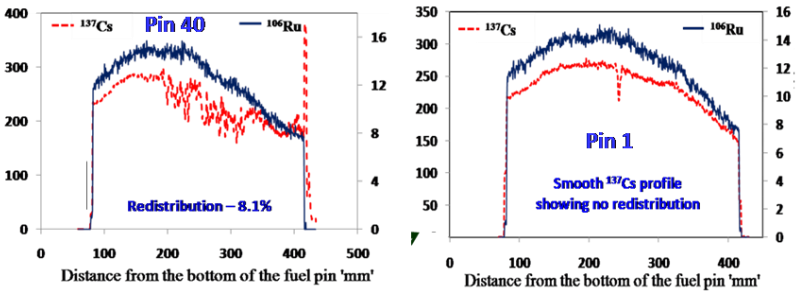

Fig 5. Axial distribution of ^{137}Cs and ^{106}Ru for fuels pins around the failed pin (refer Fig. 2 for location of the pins indicated)

Fission gas (FG) release and pressure was found to be significantly higher (17-19%, 2-2.5 MPa) in the fuel pins adjacent to the failed pin whereas those located far away showed lower gas release and pressure (8%, 0.5-1.1MPa). These observations correlated well with extensive Cs migration indicative of higher fuel temperatures in the fuel pins adjacent to failed pin. The puncturing of failed pin yielded FG of about 1 MPa pressure in the top plenum suggesting severe FCMI in the top region of fuel column above the failed region which had prevented the escape of FG through the breach.

5.4 Microstructure

The optical micrographs at the failed location revealed fuel adhering to the clad and the fuel between the circumferential crack and the clad inner diameter is seen to be highly densified. The photomicrographs at the peak power and top locations of the fuel column of the failed and adjacent intact pins show an asymmetric circumferential crack pattern indicative of non-uniform temperature around the pin (Fig. 6).

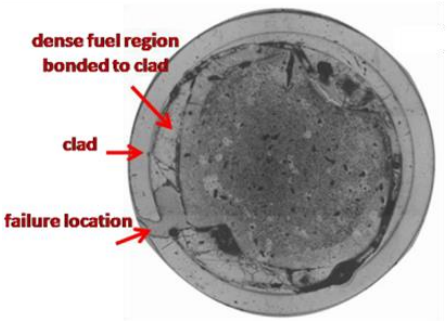

Fig. 6 Photomicrograph of the cross-sections of bottom end of failure location (240 mm from top)

Such non-uniform densification of fuel and asymmetric crack pattern were not observed in the micrographs of previously examined fuel pins. The microstructure of the clad did not show any indication of carburization on the clad inner diameter or any significant wall thinning

5.5 Hardness and tensile properties of cladding

Tensile tests on clad tube sections from different axial locations of the fuel pin adjacent to failed pin showed no evidence of severe loss of tensile strength and ductility of cladding at axial locations close to failure. The lower parts of the cladding below the peak fluence regions whose irradiation temperatures were in the range of 450-500^{0}C showed considerable hardening, with strength (UTS) of about 700-800 MPa, while the extent of hardening was significantly reduced in the sections of cladding above the fuel column with increase in irradiation temperatures to about 540-565^{0}C. The ductility of the cladding generally followed the reverse trend of strength variation showing higher values (uniform

elongation ~10%) at the upper most locations of the fuel column as compared to 4.5 % at the lower portions of the fuel column.

The microhardness measurements of the cladding at locations of failure and other axial locations did not reveal any indications of clad carburization, consistent with clad microstructure. The fractographic analysis of the failed region of the clad carried out using SEM indicated mixed mode of fracture showing both brittle and ductile features in the failure region (Fig. 7).

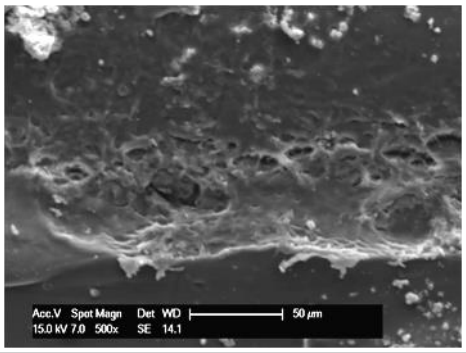

Fig. 7 SEM images of replica showing the ductile and brittle features of the failed fuel pin fracture surface indicating mixed mode failure

6.0 **Discussions and analysis of failure**

Based on the investigations, the failure of single carbide fuel pin is primarily attributed to the operating conditions of the fuel pins in this subassembly as described below. The low linear heat rating in the III ring fuel pins resulted in higher fuel swelling as compared to I ring pins. The high fuel swelling and lower clad swelling has led to severe FCMI stresses on the cladding. The higher fuel stack increase caused significant axial strain to cladding in addition to the swelling strain. This was evident from the higher length increase in III ring pins compared to I ring pins.

The local bending and distortions observed particularly in III ring fuel pins is attributed to axial stresses on the cladding, restraint of the spacer wire and interaction with adjacent pins. The increased diametral and axial strains combined with local bending could have led to coolant flow constriction between two or more adjacent pins resulting in highly localized fuel & clad temperature. Extensive cesium perturbation and higher fission gas release observed in the fuel pins adjacent to the failed pin clearly point to local temperature increase. The final clad failure in the fuel pin is attributed to FCMI generated stresses at high temperature. The fact that only one fuel pin had failed indicates the stochastic nature of failure which occurs only in pins with adverse combinations of local stress/temperature conditions and variations in fabrication tolerances [6].

7.0 Conclusions

PIE of the failed fuel subassembly offered enormous challenges due to the multidisciplinary and non-conventional nature of activities utilizing a multitude of examination techniques and correlation of results. The fuel pins of FFSA in the III ring have undergone higher fuel swelling and lower clad swelling commensurate with the operating conditions such as LHR and sodium coolant temperatures. This had led to severe FCMI stresses on the cladding. The increased diametral and axial strain combined with local bending could have led to coolant flow constriction between adjacent pins resulting in localized fuel & clad temperature increase. The higher stresses combined with higher clad temperature has resulted in failure of the clad by creep rupture.

8.0 Acknowledgements

The contributions of service groups catering to the in-cell equipments, hot cell ventilation, electrical, electronics and instrumentation systems and Non-Destructive evaluation for facilitating the PIE work is gratefully acknowledged. The support of various groups in IGCAR and other units of Department of Atomic Energy (DAE) during the failure investigation are also gratefully acknowledged.

9.0 References

[1] Baldev Raj et al., “Post Irradiation Examination of mixed (Pu,U)C fuels irradiated in the Fast Breeder Reactor”, Influence of high dose irradiation on core structural and fuel materials in advanced reactor, IAEA-TECDOC-1039, Obninsk (1997) pp.57–68.

[2] K.V.Kasiviswanathan, V.Karthik, C.N.Venkiteswaran, T.Johny, N.G. Muralidharan and Jojo Joseph Performance Assessment of Fuel and Core Structural Materials Irradiated in FBTR, Energy Procedia 7 (2011) pp.129–139.

[3] V. Karthik, Ran Vijay Kumar, A. Vijayaragavan, C.N.Venkiteswaran, V. Anandraj, P. Parameswaran, N. G. Muralidharan, S. Saroja, Jojo Joseph, K.V. Kasiviswanathan, T. Jayakumar, Baldev Raj, Characterisation of Mechanical Properties and Microstructure of Highly Irradiated SS 316, Journal of Nuclear Materials, 439 (2013), pp 224-231.

[4] C.N. Venkiteswaran, V.V. Jayaraj, B.K. Ojha, V. Anandaraj, M. Padalakshmi, S. Vinodkumar, V. Karthik, Ran Vijaykumar, A. Vijayaraghavan, R. Divakar, T. Johny, Jojo Joseph, S. Thirunavakkarasu, T. Saravanan, John Philip, B.P.C. Rao, K.V. Kasiviswanathan, T. Jayakumar, Irradiation performance of PFBR MOX fuel after 112 GWd/t burn-up, Journal of Nuclear Materials, 449 (2014) pp. 31–38.

[5] Garner, F. A. Irradiation Performance of Cladding and Structural Steels in Liquid Metal Reactors; Vol. 10A of Materials Science and Technology: A Comprehensive Treatment, VCH Publishers, 1994; Chapter 6, pp 419–543.

[6] J.R. Matthews, On the Failure of Fast Reactor Fuel Pins, Nuclear Engineering and Design 101 (1987) pp. 281-303.